

Article

Structure-activity relationships and anti-inflammatory activities of N-carbamothioylformamide analogues as MIF tautomerase inhibitors

Yu Zhang, Lei Xu, Zhiqiang Zhang, Zhiyu Zhang, Longtai Zheng, Dan Li, Youyong Li, Feng Liu, Kunqian Yu, Tingjun Hou, and Xuechu Zhen

J. Chem. Inf. Model., **Just Accepted Manuscript** • DOI: 10.1021/acs.jcim.5b00445 • Publication Date (Web): 19 Aug 2015

Downloaded from <http://pubs.acs.org> on August 25, 2015

Just Accepted

“Just Accepted” manuscripts have been peer-reviewed and accepted for publication. They are posted online prior to technical editing, formatting for publication and author proofing. The American Chemical Society provides “Just Accepted” as a free service to the research community to expedite the dissemination of scientific material as soon as possible after acceptance. “Just Accepted” manuscripts appear in full in PDF format accompanied by an HTML abstract. “Just Accepted” manuscripts have been fully peer reviewed, but should not be considered the official version of record. They are accessible to all readers and citable by the Digital Object Identifier (DOI®). “Just Accepted” is an optional service offered to authors. Therefore, the “Just Accepted” Web site may not include all articles that will be published in the journal. After a manuscript is technically edited and formatted, it will be removed from the “Just Accepted” Web site and published as an ASAP article. Note that technical editing may introduce minor changes to the manuscript text and/or graphics which could affect content, and all legal disclaimers and ethical guidelines that apply to the journal pertain. ACS cannot be held responsible for errors or consequences arising from the use of information contained in these “Just Accepted” manuscripts.

1
2
3
4 1 **Structure-activity relationships and anti-inflammatory**
5
6 2 **activities of N-carbamothioylformamide analogues as MIF**
7
8
9 3 **tautomerase inhibitors**

10
11 4 Yu Zhang^{a#}, Lei Xu^{b,c#}, Zhiqiang Zhang^a, Zhiyu Zhang^a, Longtai Zheng^a, Dan Li^b,
12
13 5 Youyong Li^d, Feng Liu^a, Kunqian Yu^e, Tingjun Hou^{a,b,d*}, Xuechu Zhen^{a*}

14
15
16 6 ^aJiangsu Key laboratory of Translational Research and Therapy for
17 7 Neuro-Psycho-Diseases & Department of Pharmacology, College of Pharmaceutical
18 8 Sciences, Soochow University, Suzhou, Jiangsu 215123, China

19
20
21 9 ^bCollege of Pharmaceutical Sciences, Zhejiang University, Hangzhou, Zhejiang
22
23 10 310058, China

24
25 11 ^cInstitute of Bioinformatics and Medical Engineering, School of Electrical and
26 12 Information Engineering, Jiangsu University of Technology, Changzhou 213001,
27 13 China.

28
29
30 14 ^dInstitute of Functional Nano & Soft Materials (FUNSOM), Soochow University,
31
32 15 Suzhou, Jiangsu 215123, China

33
34 16 ^eState Key Laboratory of Drug Research, Shanghai Institute of Materia Medica,
35
36 17 Chinese Academy of Sciences, Shanghai 200031, China

37
38
39 19 [#]Equivalent authors

40
41
42 21 **Corresponding author:**

43 22 **Xuechu Zhen**

44
45 23 E-mail: zhenxuechu@suda.edu.cn

46
47 24 Phone: +86-512-6588-0369

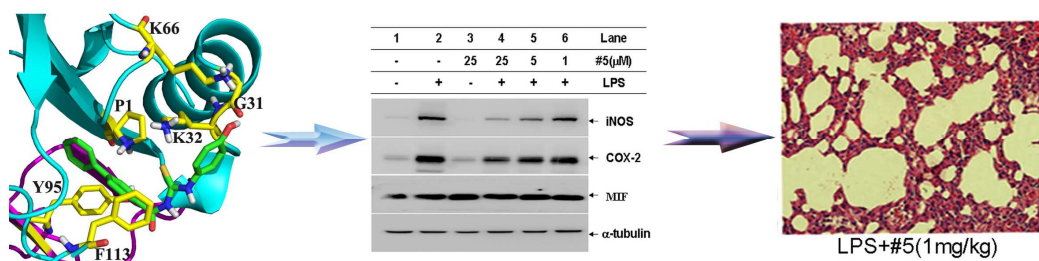
48
49 25 **Tingjun Hou**

50 26 E-mail: tingjunhou@zju.edu.cn or tingjunhou@hotmail.com

51
52 27 Phone: +86-517-8820-8412

53
54 28
55 29

For Table of Contents Use Only



Abstract

Macrophage migration inhibitory factor (MIF), a proinflammatory cytokine, is an attractive therapeutic target for the treatment of inflammatory diseases. In our previous study, 3-[(biphenyl-4-ylcarbonyl)carbamoithiyl]amino benzoic acid (compound **1**) was discovered as a potent inhibitor of MIF by docking-based virtual screening and bioassays. Here, a series of analogues of compound **1** derived from similarity search and chemical synthesis were evaluated for their MIF tautomerase activities, and their structure-activity relationships (SARs) were then analyzed. The most potent inhibitor (compound **5**) with an IC_{50} of 370 nM strongly suppressed LPS-induced production of TNF- α and IL-6 in a dose-dependent manner, and significantly enhanced the survival rate of mice with LPS-induced endotoxic shock from 0% to 35% at 0.5 mg/kg and to 45% at 1 mg/kg, highlighting the therapeutic potentials of the MIF tautomerase inhibition in inflammatory diseases.

81 Introduction

82 Macrophage migration inhibitory factor (MIF), a multi-functional protein,¹ has been
83 regarded as an attractive therapeutic target for the treatment of sepsis² and other
84 inflammatory diseases.^{3, 4} Previous studies illustrated that the inhibition of MIF
85 activity *in vivo* could attenuate the lethality of endotoxemia and sepsis in rodents.^{2, 5, 6}
86 MIF exists as a homotrimer with three identical monomers, and the catalytic active
87 site is located between two adjacent monomers of the homotrimer.⁷ In addition, MIF
88 functions as a D-dopachrome tautomerase,⁸ a phenylpyruvate tautomerase,⁹ or a
89 thiol-protein oxidoreductase.¹⁰ Despite relentless efforts, there is no clear-cut evidence
90 between the catalytic activity and biological function of MIF.¹¹ However, targeting
91 MIF tautomerase activity through small-molecule inhibitors has been proven to be an
92 attractive strategy for inhibiting MIF proinflammatory activity and attenuating its
93 biological activity *in vitro* and *in vivo*.^{11, 12}

94 To date, a variety of small-molecule MIF tautomerase inhibitors have been
95 reported by substrate analog screening, structure-based virtual screening and
96 high-throughput screening.^{1, 11, 13-15} Though these inhibitors provide a proof of
97 concept for therapeutic utility against MIF, most of them are not ideal for
98 pharmaceutical development owing to low potency or irreversible inhibition on MIF
99 tautomerase activity. For example, the prototypical MIF inhibitor ISO-1 shows only
100 micromolar potency with respect to MIF inhibition.¹⁶ The first identified MIF
101 inhibitor NAPQI,¹⁷ a metabolite of acetaminophen, forms a covalent bond with the
102 MIF N-terminal proline residue (Pro1), as well as 4-iodo-6-phenylpyrimidine
103 (4-IPP)¹⁸ and isothiocyanates (ITC).¹⁹ Recently, by combining docking-based virtual
104 screening and *in vitro* bioassays, 3-[(biphenyl-4-ylcarbonyl)carbamothioyl]amino
105 benzoic acid (presented as compound **1** in this study) was identified to be a
106 competitive inhibitor of MIF (IC₅₀ = 550 nM), and was found to effectively inhibit the
107 biological functions of MIF.²⁰ However, the structure-activity relationships (SARs) of
108 the analogues of compound **1** have not been characterized and its *in vivo* potency has
109 not been tested. Therefore, in this study, a number of analogues of compound **1** were

1
2
3
4 110 purchased or chemically synthesized, and their MIF tautomerase activities were
5
6 111 evaluated. In total, 31 compounds were found to be potent tautomerase inhibitors of
7
8 112 MIF with IC_{50} values below 10 μ M (six with $IC_{50} < 1 \mu$ M). The strong
9
10 113 anti-inflammatory potency of the most potent inhibitor, compound **5** ($IC_{50} = 370$ nM),
11
12 114 as evidenced by suppressing lipopolysaccharide (LPS)-induced macrophage
13
14 115 activation *in vitro*, was verified by ELISA, quantitative real-time PCR and western
15
16 116 blot. Furthermore, the therapeutic importance of the MIF inhibition by compound **5**
17
18 117 was demonstrated by increasing the survival rate of mice with LPS-induced endotoxic
19
20 118 shock from 0% to 35% at 0.5 mg/kg and to 45% at 1 mg/kg, respectively.
21
22 119

22 **Materials and Methods**

23 **Analogues Chosen by Similarity Search and Molecular Docking**

24
25 121
26 122 Because the commercial chemical databases are usually enriched with analogues by
27
28 123 the nature of their synthetic routes, the analogues of compound **1** were identified from
29
30 124 the ChemBridge and Specs databases by similarity search based on the Tanimoto
31
32 125 similarity coefficients²¹ computed from the MACCS Structural fingerprints in MOE.²²
33
34 126 Tanimoto similarity coefficients higher than 0.85 and 0.80 were set as the cutoffs for
35
36 127 the ChemBridge and Specs databases, respectively.

37
38 128 Then, the molecules selected by similarity search were processed with the
39
40 129 program LigPrep in Schrödinger²³ to generate the tautomers and protonation states at
41
42 130 pH = 7.4 (up to 30 stereoisomers for each compound with chiral centers), and then
43
44 131 docked into the binding site of MIF. The crystal structure of MIF complexed with
45
46 132 *p*-hydroxyphenyl pyruvate (HPP) (PDB entry: 1CA7)²⁴ was selected as the template
47
48 133 for molecular docking. The ligand located in the active site between chain A and
49
50 134 chain B was retained, and the other two ligands were deleted. The N-terminal proline
51
52 135 residue (P1) was protonated in terms of the experimental measurement and theoretical
53
54 136 calculations.^{25, 26} Hydrogen and other missing atoms were added, and the protein was
55
56 137 energy-minimized using OPLS2005 force field²⁷ with the Protein Preparation Wizard
57
58 138 module in Schrödinger (version 9.0). All structures were docked into the active site of

1
2
3 139 MIF and scored by the extra precision (XP) scoring function of Glide. In the docking
4
5 140 process of Glide, the protein conformation is fixed and each docked ligand is flexible.
6
7 141 As for the grid generation and ligand docking, the default Glide settings were
8
9 142 employed. The top scored molecules were assessed by the REOS rules²⁸ and the
10
11 143 drug-likeness filters developed in our group²⁹⁻³¹ to remove compounds with toxic,
12
13 144 reactive or otherwise undesirable moieties, and finally 46 compounds were chosen
14
15 145 and purchased.

16
17 146

18 147 **Synthetic Chemistry**

19
20 148 The importance of the halogen substitution on MIF tautomerase activity has been
21
22 149 reported in the previous study, where the substitution of mono-fluorination onto the
23
24 150 *ortho* position of the phenolic group of ISO-1 could improve the inhibition activity
25
26 151 against MIF up to 41%.³² In order to study the effect of the halogen substitution on
27
28 152 bioactivity, 11 analogues of compound **1** were synthesized. ¹H NMR and ¹³C NMR
29
30 153 spectra were acquired on 400 MHz (Varian) spectrometers. Chemical shifts were
31
32 154 given in ppm through tetramethylsilane (TMS) as internal standard. At last, the
33
34 155 compounds were purified using silica gel 100-200 mesh for column chromatography.
35
36 156 The synthetic routes for the pursued series are depicted in Schemes 1-2. A mixture of
37
38 157 4-Bromobenzoic Acid Methyl Ester (645 mg, 3.0 mmol, 1.0 eq.), aryl boronic acid
39
40 158 (3.6 mmol, 1.2 eq.), Pd(PPh₃)₄ (69 mg, 0.05 mmol, 0.02 eq.), and Na₂CO₃ (699 mg,
41
42 159 6.6 mmol, 2.2 eq.) in dioxane/H₂O (7:1, v/v) (16 mL) was stirred at 100 °C for 1 h.
43
44 160 The solvent was removed under reduced pressure and the residue was diluted with
45
46 161 water (10 mL) and extracted with EtOAc (3 × 10 mL). The combined organic extracts
47
48 162 were washed with brine, dried over Na₂SO₄, filtered and concentrated. The residue
49
50 163 was purified by flash column chromatography (hexane/EtOAc 50:1) to give the
51
52 164 corresponding ester. A solution of unsaturated acids (2 mmol) in dichloromethane (10
53
54 165 mL) was added oxalyl chloride (1.02 g, 8 mmol), followed by adding 2 drops of DMF.
55
56 166 The mixture was stirred at room temperature for 1 h, and then excess oxalyl chloride
57
58 167 and dichloromethane were removed *in vacuo* to provide crude acyl chloride. A
59
60 168 suspension of benzoyl chloride (3 mmol) and sodium thiocyanate (486 mg, 6 mmol)

1
2
3 169 in acetonitrile (9 ml) was stirred for 1 h at room temperature. Then, sodium chloride
4
5 170 was filtered, and anthranilic acid was added to the filtrate. The mixture was stirred for
6
7 171 1-2 h, methanol (10 ml) was added to the solvent and stirred for 10 min, and then the
8
9 172 solvent was filtrated and the solid was collected. The detailed spectral data are
10
11 173 provided at Part 1 of the Supporting Information.

12
13 174 In total, there are 51 compounds in Tables 1~3. Compound 1 is the lead
14
15 175 compound identified from our previous study,²⁰ compounds 2-11, 15-34 and 43-51
16
17 176 were purchased from the ChemBridge and Specs databases, and the others were
18
19 177 chemically synthesized.

20
21 178

22 179 **Assay for MIF Tautomerase Activity**

23
24 180 The following protocol was adapted from Tao *et al.*³³ Fresh solution of L-dopachrome
25
26 181 methyl ester was prepared by mixing equal volumes of L-3,4-dihydroxyphenylalanine
27
28 182 methyl ester (6 mM), sodium metaperiodate (12 mM) and incubated for 20 min at
29
30 183 room temperature. The dopachrome solution was prepared before the inhibition assay
31
32 184 owing to its relative instability. Then, hMIF (120 nM) was added to a 96-well plate
33
34 185 containing L-dopachrome (30 μ L) in 10 mM potassium phosphate buffer and 0.5 mM
35
36 186 EDTA at pH = 6.2. The inhibitory effect of each compound against the tautomerase
37
38 187 activity of MIF was measured by adding various concentrations of the compound to
39
40 188 the 96-well plate containing hMIF (120 nM) and incubating for 30 min followed by
41
42 189 the addition of L-dopachrome methyl ester. The absorbance was measured by
43
44 190 monitoring the decrease in absorbance at 475 nm for 3 min with a Tecan Infinite
45
46 191 M1000 microplate reader (Tecan Group Ltd.).

47 192

48 193 **Cell Culture and Cell Viability Assay**

49
50 194 The RAW 264.7 cell line was purchased from the American Type Culture Collection
51
52 195 (ATCC). The cells were maintained in complete DMEM supplemented with 10%
53
54 196 heat-inactivated fetal bovine serum, penicillin (100 U/mL), and streptomycin (100
55
56 197 mg/mL) in a 37 °C, 5% CO₂ incubator. The cells were attached to the culture plate at
57
58 198 least for 24 h prior to allowing various experiments. Cell viability was determined by

1
2
3 199 3-(4,5-dimethylthiazol-2-yl)-2,5-diphenyltetrazolium bromide (MTT) assay. RAW
4
5 200 264.7 macrophages were seeded into 96-well plates (5×10^4 cells/well). After
6
7 201 appropriate treatment, the cells were incubated in MTT solution at 37 °C for 4 h, and
8
9 202 then 100 μ L of DMSO was added to each well to dissolve the violet formazan crystals
10
11 203 for 5 min as previously described¹⁸. The optical density was measured at 540 nm on a
12
13 204 Microplate Reader (Infinite M200 PRO, Tecan, Switzerland).
14
15

16 **Measurement of Intracellular Nitric Oxide (NO)**

17
18 207 RAW 264.7 macrophages were seeded into 96-well plates, and culture supernatants
19
20 208 were collected after treatment with LPS or compounds. Concentration of NO was then
21
22 209 determined by using the Griess reagent as described previously.³⁴ Briefly fifty
23
24 210 microliters of Griess reagent (containing 0.2% w/v N-(1-naphthyl) ethylenediamine
25
26 211 dihydrochloride and 2% w/v sulfanilamide in 5% v/v H₃PO₄) were mixed with same
27
28 212 volumes of cell culture conditioned medium, and then incubated at room temperature
29
30 213 for 10 min in the dark. The absorbance of mixture was measured by a 96-well
31
32 214 microplate reader (Tecan Systems, Inc.) at 570 nm.
33
34

35 **Enzyme-linked Immunosorbent Assay (ELISA)**

36
37 217 The levels of TNF- α and IL-6 in the cell culture medium were determined by specific
38
39 218 ELISA kits according to the manufacturer's instructions.³⁵
40
41

42 **RNA Extraction and Real-time Quantitative PCR (RT-qPCR)**

43
44 221 Total RNA was extracted using the TRIzol reagent according to its manufacturer's
45
46 222 instructions (TaKaRa, Dalian, China). The obtained total RNA was used for synthesis
47
48 223 of cDNA using the ImProm-IITM Reverse Transcription System (Promega, USA).
49
50 224 Quantitative real time PCR was performed using Maxima SYBR Green/ROX qPCR
51
52 225 Master Mix. The specific primers used for cDNA amplification are following: iNOS
53
54 226 forward, CAG GAG GAG AGA GAT CCG ATT TA, and iNOS reverse, GCA TTA
55
56 227 GCA TGG AAG CAA AGA; TNF- α forward, CAT CTT CTC AAA ATT CGA GTG
57
58 228 ACA A, and TNF- α reverse, TGG GAG TAG ACA AGG TAC AAC CC; IL-1 β
59
60

1
2
3 229 forward, TCC AGG ATG AGG ACA TGA GCA C, and IL-1 β reverse, GAA CGT
4
5 230 CAC ACA CCA GCA GGT TA; GAPDH forward, TGT GTC CGT CGT GGA TCT
6
7 231 GA, and GAPDH reverse, TTG CTG TTG AAG TCG CAG GAG; MIF forward,
8
9 232 CGT GCC AGA GGG GTT TCT GT, and MIF reverse, GTT CTG GGC ACC ACC
10
11 233 GAT CT; HO-1 forward, CAC GCA TAT ACC CGC TAC CT, and HO-1 reverse, TCT
12
13 234 GTC ACC CTG TGC TTG AC. The relative level of gene expression was normalized
14
15 235 to the level of GAPDH and calculated using the $2^{-(\Delta\Delta CT)}$ formula.
16
17 236

18 237 **Western Blot Analysis**

19
20 238 After appropriate treatment, RAW 264.7 macrophages were collected and washed
21
22 239 three times with ice-cold PBS. And the cells were lysed with RIPA lysis buffer [50
23
24 240 mM Tris [pH 8], 1% Triton X-100, 0.1% SDS, 0.5% sodium deoxycholate, 150 mM
25
26 241 NaCl and a protease inhibitor cocktail (Roche Boehringer Mannheim Diagnostics,
27
28 242 Mannheim, Germany)]. Protein concentration was measured with protein extraction
29
30 243 kit and BCA protein assay kit (Bio-Rad, Hercules, CA). The samples were boiled for
31
32 244 5 min which contained 1% β -mercaptoethanol followed by separation with
33
34 245 SDS-PAGE, then the proteins were transferred to polyvinylidene difluoride (PVDF)
35
36 246 membranes (Millipore, Billerica, MA), blocked in PBS-T (PBS plus 0.1% Tween-20)
37
38 247 containing 5% skim milk at room temperature for 90 min. The membrane was probed
39
40 248 with primary antibodies [polyclonal rabbit anti-mouse iNOS (Abcam, NT); polyclonal
41
42 249 rabbit anti-mouse COX-2(Santa Cruz Biotechnology); monoclonal anti-rabbit MIF
43
44 250 (Abcam, NT); and monoclonal anti-a-tubulin mouse ascites fluid (Sigma)] at 4 °C
45
46 251 overnight. After washing the membrane with PBS-T, the membrane was incubated
47
48 252 with HRP-conjugated secondary antibodies (Sigma-Aldrich) at room temperature for
49
50 253 90 min respectively. The protein bands were visualised using enhanced
51
52 254 chemiluminescence (ECL) (Pierce Biotechnology Inc., Rockford, IL), with a
53
54 255 ChemiScope 3300 Mini (CLINX, Shanghai, China) and the relative signal intensity
55
56 256 was quantified by densitometric analysis (Quantity One).
57
58 257

58 258 **Experimental Endotoxic Shock Model**

1
2
3 259 LPS (Escherichia coli 0111: B4, Catalog no.L-2630, Lot no.78H4086, Sigma–Aldrich,
4
5 260 St. Louis, MO, USA) was dissolved in saline for administration to C57 BALB/c mice.
6
7 261 Mice were injected intraperitoneally with LPS at a dose of 4.5 mg/kg and in the
8
9 262 volume of 0.1 ml/10g body weight to induce endotoxin shock model. Mice received
10
11 263 intraperitoneal administrations of compound **5** (0.5 mg/kg or 1 mg/kg) which prepared
12
13 264 in 2% dimethyl sulfoxide/2% Tween 80/2% Cremophor EL in saline either or vehicle
14
15 265 1 h prior to LPS injection. Survival was monitored at 1, 2, 3, 4, 5 and 6 days post-LPS
16
17 266 challenge. The number of animals used in each experimental group was 20. The mice
18
19 267 that survived over 6 days were euthanized by cervical dislocation. All experimental
20
21 268 procedures utilizing mice were in accordance with National Institute of Health
22
23 269 guidelines. The animal study was approved by the Institutional Review Board of
24
25 270 Soochow University.

26
27
28 271

28 272 **Histological and Statistical Analysis**

29
30 273 The lung tissues were collected at 12 h after LPS challenge for histological
31
32 274 assessment. Lung tissues were fixed in formalin and subsequently embedded in
33
34 275 paraffin then stained with hematoxylin & eosin (H.E) for histopathological evaluation
35
36 276 under light microscope (Olympus, Japan). Results were expressed as the mean \pm SD
37
38 277 using GraphPad Prism 5.0. One-way ANOVAs followed by Bonferroni tests were
39
40 278 utilized for multiple-group comparisons. A value of $p < 0.05$ was considered
41
42 279 statistically significant.

43
44
45 280

45 281 **Results and Discussion**

47 282 **SAR Analyses for Analogues of Compound 1**

49
50 283 The commercial chemical databases are usually enriched with analogues by the nature
51
52 284 of their synthetic routes, and therefore, in this study, based on similarity search and
53
54 285 molecular docking, 16 analogues from ChemBridge and 30 analogues from Specs
55
56 286 were purchased for biological assays.

57 287 Seven out of the 46 compounds were not tested owing to poor solubility in

1
2
3 288 DMSO/ethanol/water, and the other compounds were then assayed for their MIF
4
5 289 tautomerase activities with L-dopachrome as the substrate. The prototypical MIF
6
7 290 inhibitor (compound **1**), our previously reported tautomerase inhibitor of MIF,²⁰ was
8
9 291 used as the reference control, and DMSO (1%, v/v) used as the vehicle control. The *in*
10
11 292 *vitro* MIF tautomerase assay showed that 28 analogues have IC₅₀ values below 10 μM
12
13 293 and 5 below 1 μM. All these compounds had one common key structural feature: two
14
15 294 aromatic rings linked by *N*-carbamothioylformamide in the middle position.
16
17 295 According to the structural differences, these analogues could be roughly classified
18
19 296 into three categories (Tables 1~3): analogues with biphenyl (**2-11**), analogues with
20
21 297 benzene (**15-34**) and analogues with diphenylmethane (**43-51**). The SAR analyses of
22
23 298 these compounds could provide important insights of the essential structural features
24
25 299 for effective MIF inhibitors.

26 300 Analyses of the 10 compounds in Table 1 illustrated some noteworthy
27
28 301 observations of the SARs: (1) the substitution of the carboxy group on *R*₂ was critical,
29
30 302 and the MIF inhibitory activity became worse when the position of carboxy was
31
32 303 changed from *meta* to *para* (**1 vs 3**); (2) the introduction of a chlorine atom (*R*₄)
33
34 304 slightly promoted the potency (**1 vs 8**), and the replacement of chlorine with the
35
36 305 methyl or methoxyl group decreased the potency, which might be explained by the the
37
38 306 changes in the density distribution of the electron cloud of the benzene ring resulted
39
40 307 from electron-withdrawing group in comparison with electron-donating group (**2, 8**
41
42 308 and **10**); (3) when only *R*₃ was changed by replacing the hydrogen atom with the
43
44 309 hydroxy, acetylamino, carboxy or carbomethoxy group, the activity decreased
45
46 310 significantly (**5, 4, 3 and 6**), for instance, compound **5** showed the best MIF inhibitory
47
48 311 potency. Thus, the introduction of hydroxy on *R*₂ could enhance the inhibitory activity
49
50 312 on MIF.

51 313 In addition, the key observations of the SARs from the 20 compounds in Table 2
52
53 314 were summarized as follows: (1) upon the replacement of hydrogen with a methyl
54
55 315 group on *R*₆, improvement of the inhibitory activity was observed (**16 vs 18**).
56
57 316 Moreover, the position of methyl had substantial influence on the inhibitory activity,
58
59 317 and the potency increased from *meta* to *para* (**16 vs 20**) while strongly decreased to

1
2
3
4 318 *ortho* (**23** vs **24**); (2) when only R_3 was changed by replacing hydrogen with the acetyl,
5
6 319 carbomethoxy, carboxy or carbethoxy group, the activity decreased gradually (**25**, **24**,
7
8 320 **18** and **28**), and thus the introduction of acetyl on R_3 might be beneficial to the
9
10 321 potency on MIF inhibition; (3) the substitution of carbomethoxy on R_1 was important
11
12 322 for the inhibitory activity (compounds **33** and **34** with the IC_{50} values below 1 μM),
13
14 323 and when only R_3 was changed, the potency increased upon the replacement of
15
16 324 carboxy with the carbomethoxy group (**18** vs **24**). Generally, the introduction of the
17
18 325 carbomethoxy group was beneficial to the potency, in particular on R_1 .

19
20 326 Analyses of the 9 compounds in Table 3 exhibited some interesting observations
21
22 327 of the SARs: (1) the substitution of carbomethoxy was beneficial, and compound **46**
23
24 328 with carbomethoxy at the *para* position showed better inhibition than the
25
26 329 corresponding analogue **49** with carbomethoxy at the *ortho* position; (2) when only R_3
27
28 330 was changed by replacing hydrogen with the phenylamino, benzamido, carbomethoxy,
29
30 331 carboxy or formylamino group, the activity decreased gradually (**51**, **47**, **46**, **43** and
31
32 332 **48**). Generally, the substituents of the aromatic group on R_3 were critical to the
33
34 333 potency (**47** and **51**).

35
36 334 To determine the activity affected by the substitution of halogen atom, 11
37
38 335 compounds were synthesized and assayed for the MIF tautomerase inhibitory
39
40 336 activities. As shown in Tables 1 and 2, the introductions of the fluorine atoms on R_5
41
42 337 and R_6 showed unfavorable effect on the inhibitory activity in comparison with the
43
44 338 chlorine atoms (**13** vs **14**), as well as the trifluoromethyl group (**12** vs **13**).
45
46 339 Accordingly, we speculated that the introduction of the trichloromethyl group on R_5
47
48 340 and R_6 might be favorable to the inhibitory activity. In addition, the position of the
49
50 341 fluorine atom had significant impact on the MIF inhibitory activity, and the potency
51
52 342 dramatically increased from *ortho* to *para* to *meta* (**42**, **38** and **39**). Consequently, the
53
54 343 introduction of the fluorine atom on R_5 might be beneficial, whereas the introduction
55
56 344 of the fluorine atom on R_4 resulted in a dramatic loss of the inhibitory activity. The
57
58 345 potency gradually increased with the substitution of the fluorine, chlorine or bromine
59
60 346 atom, respectively (**38**, **37** and **35**), which might be explained by the inductive effect
347 that lead to the changes in the density distribution of the electron cloud of the benzene

1
2
3 348 ring, thereby making strong π - π interaction with Tyr95 and Phe113.
4
5
6

349

350 **Predicted Binding Poses of Four Most Potent Inhibitors**

351 The most potent inhibitor (compound **5**) possesses a hydroxyl group at the *para*
352 position, in comparison with the carboxyl group at the *meta* position of the other three
353 compounds (**8**, **13** and **15**). As shown in Figure 1a, the biphenyl group of compound **5**
354 could form the aryl-aryl interaction with Tyr95 and Phe113, and the cation- π
355 interaction with the protonated Pro1 (Figure 1a). In addition, the hydroxyl group of
356 compound **5** could form the H-bonds with Gly31 and Lys66, and the hydrophobic
357 interaction with Pro1, Trp108 and Phe113. Compounds **8** and **13** were the chlorine
358 derivatives of compound **1**, though one substitutes in the benzoic acid side chain and
359 the other in the biphenyl group. The modeling results suggested that their docked
360 poses were quite similar, and their biphenyl rings were stabilized in a T-shaped
361 geometry by forming a network of the π - π interactions with Tyr95 and Phe113. The
362 carboxyl group of compound **8** was predicted to form the H-bonds with Lys32 and
363 Lys66, and compound **13** formed the cation- π interaction with the protonated Pro1.
364 Compared with the other three compounds (**5**, **8** and **13**), compound **15** had a phenyl
365 group rather than a biphenyl side chain. However, its activity ($IC_{50} = 660$ nM) was
366 improved slightly in comparison with that of compound **1** with the biphenyl group
367 ($IC_{50} = 720$ nM), and its carbonyl group was predicted to form the H-bonds with the
368 basic residues Lys32 and Lys66. Accordingly, we speculated that if the biphenyl
369 group of compound **5** was substituted by the benzyl group, and the chlorine atom was
370 introduced at the *para* position of the hydroxyl group, its potency might be promoted.

371

372 **Biological Activities**

373 As an important proinflammatory cytokine, MIF can induce the secretion of itself and
374 other proinflammatory cytokines such as TNF- α , IL-1b, IL-6, and IL-8, and stimulate
375 NO production.^{36, 37} Expression studies also identified that MIF secretion could be
376 induced by LPS, TNF- α and IFN- γ in RAW 264.7 macrophages.³⁸ A separate line of
377 investigation implicated a strong relationship between the specific inhibition of MIF

1
2
3 378 tautomerase activity and suppression of MIF proinflammatory activities, such as
4
5 379 ISO-1 that could reduce inflammation induced by MIF.^{11, 16} It was also reported that
6
7 380 inhibition of MIF tautomerase activity not only suppressed MIF induced production
8
9 381 of proinflammatory cytokines but also reduced LPS- triggered inflammatory
10
11 382 responses *in vitro* and *in vivo*.^{6, 39} Therefore, we investigated the anti-inflammatory
12
13 383 effects of MIF tautomerase inhibitors on LPS-induced macrophage. Over-production
14
15 384 of NO has been used as a hallmark of inflammatory activation in LPS-treated
16
17 385 macrophage.⁴⁰ Thus, we examined the effect of inhibitors of MIF enzymatic activity
18
19 386 on NO production in LPS-induced RAW 264.7 cells. All compounds with potent
20
21 387 tautomerase activities ($IC_{50} < 10 \mu M$) could attenuate LPS-stimulated NO production,
22
23 388 and three of them with $IC_{50} < 720 \text{ nM}$ exhibited the highest potency (Table 1 and
24
25 389 Figure 2). LPS markedly increased TNF- α and iNOS expression, which was
26
27 390 significantly inhibited by respective compound among them, compound 5 exhibited
28
29 391 the most potent activity. (Figure 2e-2f). Therefore, we focused on the
30
31 392 anti-inflammatory activity of compound 5 in the following experiments.

32
33 393 To further test the anti-inflammatory effect of compound 5, the production of NO,
34
35 394 TNF- α and IL-6 were measured from LPS -induced in RAW 264.7 macrophage in the
36
37 395 presence or absence of compound 5. As shown in Figure 3, compound 5 strongly
38
39 396 inhibited NO production in LPS-stimulated RAW 264.7 in a dose-dependent manner
40
41 397 (Figure 3a). To exclude the possibility that the decrease of NO was due to cell death,
42
43 398 the cell viability was measured by MTT assay. Results showed that compound 5 at the
44
45 399 indicated concentrations (1-25 μM) did not alter the cell viability (Figure 3b). TNF- α
46
47 400 and IL-6 are proinflammatory cytokines that can initiate the inflammatory response
48
49 401 and mediate the development of chronic inflammatory diseases.^{41, 42} The productions
50
51 402 of TNF- α and IL-6 in the culture supernatants were measured by ELISA. In
52
53 403 agreement with the results of NO, compound 5 markedly inhibited LPS-induced
54
55 404 production of TNF- α and IL-6 in a dose-dependent manner (Figure 3c-3d).

56
57 405 Next, we measured the gene and protein expression of those proinflammatory
58
59 406 cytokines in RAW264.7 macrophages. As shown in Figure 4a-4e, compound 5 could
60
407 dramatically inhibit the gene expression of iNOS, IL-6, TNF- α , COX-2, and IL-1b in

1
2
3 408 a dose-dependent manner in LPS-stimulated RAW 264.7 macrophages. Recent study
4
5 409 suggested that HO-1 was one of the key defense molecules against LPS-induced
6
7 410 sepsis and HO-1 overexpression could protect against the systemic inflammatory
8
9 411 response.⁴³⁻⁴⁶ To determine whether compound **5** could attenuate inflammatory
10
11 412 response by inducing HO-1 expression, the HO-1 mRNA expression levels were also
12
13 413 measured. LPS resulted in an increase in HO-1 mRNA levels, and pretreatment with
14
15 414 compound **5** (25 μ M) for 30 min before LPS further increased HO-1 protein levels
16
17 415 (Figure 4f). In accordance with the mRNA expression, compound **5** also suppressed
18
19 416 LPS-induced iNOS, COX-2 expression in a dose-dependent manner in RAW 264.7
20
21 417 macrophages without altering MIF protein level (Figure 4g).

418

419 **Compound 5 elicits protection from LPS-induced Endotoxic Shock in mice.**

22
23
24 419
25
26 420 Many studies have demonstrated that anti-MIF antibodies or MIF inhibitors could
27
28 421 attenuate inflammatory cascade and improve the survival rate in sepsis.^{2, 38, 47, 48} To
29
30 422 determine whether compound **5** also produced anti-inflammatory activity *in vivo*,
31
32 423 LPS-induced experimental shock mouse model was employed. As shown in Figure 5a,
33
34 424 application of compound **5** could protect the BALB/c mice from endotoxic shock, as
35
36 425 evidenced by increasing the survival rate of mice from 0% to 35% at 0.5 mg/kg and to
37
38 426 45% at 1 mg/kg. It is known that LPS induces dramatic increases in inflammation
39
40 427 cytokines, such as TNF- α and IL-6, and results in severe tissue damage, multiple
41
42 428 organ failure and eventually leading to death in sepsis.^{49, 50} We found that compound
43
44 429 **5** significantly decreased the serum levels of TNF- α and IL-6 in LPS-induced
45
46 430 endotoxin model. These results clearly indicated that compound **5** attenuated
47
48 431 inflammatory responses in LPS-induced sepsis mice by inhibiting the secretion of
49
50 432 proinflammatory cytokines. Tissue injury, especially lung, is a main cause of mortality
51
52 433 in LPS-induced sepsis.⁵¹ Therefore, the lungs were examined histologically at the
53
54 434 points of 12 h after LPS treatment with or without compound **5** (1, 0.5 mg/kg, i.p.) 1 h
55
56 435 pretreatment. Histopathology of the lung sections were illustrated in Figure 5d.
57
58 436 Vehicle group showed integrate and clear alveolar spaces, while LPS alone treatment
59
60 437 showed an acute inflammatory response including infiltration of inflammatory cells,

1
2
3 438 alveolar septum thickness, and swelling of the alveolar wall. However, the lung injury
4
5 439 was significantly alleviated in the mice with compound **5** (1, 0.5 mg/kg) pretreated
6
7 440 group. These findings highlighted that compound **5** reduced the mortality through
8
9 441 improving inflammatory responses.
10

11 442

12 13 14 443 **Conclusion**

15
16 444 In this study, the SARs for the 50 analogues of N-carbamothioylformamide were
17
18 445 analyzed. The results provided valuable information about the essential structural
19
20 446 features of effective MIF inhibitors. We further studied the biological functions of
21
22 447 compound **5**, the most potent MIF inhibitor with $IC_{50} = 370$ nM, in anti-inflammatory
23
24 448 responses both *in vitro* and *in vivo*. The present data illustrated that targeting the
25
26 449 tautomerase active site of MIF by small-molecule inhibitors was an attractive strategy
27
28 450 for therapeutic interventions in the inflammatory diseases such as sepsis.
29

30 451

31 452 **Acknowledgment**

32
33 453 This study was supported by the National Science Foundation of China (21173156,
34
35 454 81130023, 81373382, 81372688 and 21302134), the National Basic Research
36
37 455 Program of China (973 program, 2012CB932600 and 2011CB5C4403). Supports
38
39 456 from Priority Academic Program Development of Jiangsu Higher Education Institutes
40
41 457 (PAPD), Project Funded by China Postdoctoral Science Foundation and Grant from
42
43 458 Jiangsu Science and Technology Commission (BY2011131) are also appreciated.
44

45 459

46 460 **Supporting Information**

47
48
49 461 **Part 1.** The detailed spectral data for Compounds **12~14** and **35~42**; **Table S1**. The
50
51 462 number, docking score, source of database and IDs for the compounds shown in
52
53 463 Tables 1~3 from similarity search. This material is available free of charge via the
54
55 464 Internet at <http://pubs.acs.org>.
56

57 465
58
59
60

466 **References**

- 467 1. Xu, L.; Li, Y. Y.; Sun, H. Y.; Zhen, X. C.; Qiao, C. H.; Tian, S.; Hou, T. J., Current
468 Developments of Macrophage Migration Inhibitory Factor (MIF) Inhibitors. *Drug Discov. Today*
469 **2013**, *18*, 592-600.
- 470 2. Al-Abed, Y.; Dabideen, D.; Aljabari, B.; Valster, A.; Messmer, D.; Ochani, M.; Tanovic, M.;
471 Ochani, K.; Bacher, M.; Nicoletti, F.; Metz, C.; Pavlov, V. A.; Miller, E. J.; Tracey, K. J., ISO-1
472 Binding to the Tautomerase Active Site of MIF Inhibits its Pro-inflammatory Activity and
473 Increases Survival in Severe Sepsis. *J. Biol. Chem.* **2005**, *280*, 36541-36544.
- 474 3. Morand, E. F.; Leech, M.; Bernhagen, J., MIF: a New Cytokine Link between Rheumatoid
475 Arthritis and Atherosclerosis. *Nature Rev. Drug. Discov.* **2006**, *5*, 399-411.
- 476 4. Flaster, H.; Bernhagen, J.; Calandra, T.; Bucala, R., The Macrophage Migration Inhibitory
477 Factor-glucocorticoid Dyad: Regulation of Inflammation and Immunity. *Mol. Endocrinol.* **2007**,
478 *21*, 1267-1280.
- 479 5. Calandra, T.; Echtenacher, B.; Le Roy, D.; Pugin, J.; Metz, C. N.; Hultner, L.; Heumann, D.;
480 Mannel, D.; Bucala, R.; Glauser, M. P., Protection from Septic Shock by Neutralization of
481 Macrophage Migration Inhibitory Factor. *Nature Med.* **2000**, *6*, 164-170.
- 482 6. Dabideen, D. R.; Cheng, K. F.; Aljabari, B.; Miller, E. J.; Pavlov, V. A.; Al-Abed, Y., Phenolic
483 Hydrazones are Potent Inhibitors of Macrophage Migration Inhibitory Factor Proinflammatory
484 Activity and Survival Improving Agents in Sepsis. *J. Med. Chem.* **2007**, *50*, 1993-1997.
- 485 7. Sun, H.; Bernhagen, J.; Bucala, R.; Lolis, E., Crystal Structure at 2.6 Å Resolution of Human
486 Macrophage Migration Inhibitory Factor. *Proc. Natl. Acad. Sci. U.S.A.* **1996**, *93*, 5191-5196.
- 487 8. Sugimoto, H. T., M.; Nakagawa, A.; Tanaka, I.; Suzuki, M.; Nishihira, J., Crystal Structure of
488 Human D-dopachrome Tautomerase, a Homologue of Macrophage Migration Inhibitory Factor, at
489 1.54 Å Resolution. *Biochemistry* **1999**, *38*, 3268-3279.
- 490 9. Rosengren, E. Å., P.; Thelin, S.; Hansson, C.; Ahlfors, S.; Björk, P. J., L.; Rorsman, H.; Åman,
491 P.; Thelin, S.; Hansson, C.; Ahlfors, S.; Björk, P.; Jacobsson, L.; Rorsman, H., The Macrophage
492 Migration Inhibitory Factor MIF is a Phenylpyruvate Tautomerase. *FEBS Lett.* **1997**, *417*, 85-88.
- 493 10. Kleemann, R.; Kapurniotu, A.; Frank, R. W.; Gessner, A.; Mischke, R.; Flieger, O.; Jüttner, S.;
494 Brunner, H.; Bernhagen, J., Disulfide Analysis Reveals a Role for Macrophage Migration
495 Inhibitory Factor (MIF) as Thiol-protein Oxidoreductase. *J. Mol. Biol.* **1998**, *280*, 85-102.
- 496 11. Garai, J.; Lorand, T., Macrophage Migration Inhibitory Factor (MIF) Tautomerase Inhibitors as
497 Potential Novel Anti-inflammatory Agents: Current Developments. *Curr. Med Chem.* **2009**, *16*,
498 1091-1114.
- 499 12. Cournia, Z.; Leng, L.; Gandavadi, S.; Du, X.; Bucala, R.; Jorgensen, W. L., Discovery of Human
500 Macrophage Migration Inhibitory Factor (MIF)-CD74 Antagonists via Virtual Screening. *J. Med.*
501 *Chem.* **2009**, *52*, 416-424.
- 502 13. Ouertatani-Sakouhi, H.; El-Turk, F.; Fauvet, B.; Cho, M.-K.; Karpinar, D. P.; Le Roy, D.; Dewor,
503 M.; Roger, T.; Bernhagen, J.; Calandra, T.; Zweckstetter, M.; Lashuel, H. A., Identification and
504 Characterization of Novel Classes of Macrophage Migration Inhibitory Factor (MIF) Inhibitors
505 with Distinct Mechanisms of Action. *J. Biol. Chem.* **2010**, *285*, 26581-26598.
- 506 14. Pantouris, G.; Rajasekaran, D.; Garcia, A. B.; Ruiz, V. G.; Leng, L.; Jorgensen, W. L.; Bucala, R.;
507 Lolis, E. J., Crystallographic and Receptor Binding Characterization of Plasmodium Falciparum
508 Macrophage Migration Inhibitory Factor Complexed to Two Potent Inhibitors. *J. Med. Chem.*

- 1
2
3 509 2014, 57, 8652-8656.
- 4 510 15. Dahlgren, M. K.; Garcia, A. B.; Hare, A. A.; Tirado-Rives, J.; Leng, L.; Bucala, R.; Jorgensen,
5 511 W. L., Virtual Screening and Optimization Yield Low-Nanomolar Inhibitors of the Tautomerase
6 512 Activity of Plasmodium falciparum Macrophage Migration Inhibitory Factor. *J. Med. Chem.*
7 513 2012, 55, 10148-10159.
- 8 514 16. Lubetsky, J. B.; Dios, A.; Han, J. L.; Aljabari, B.; Ruzsicska, B.; Mitchell, R.; Lolis, E.; Al-Abed,
9 515 Y., The Tautomerase Active Site of Macrophage Migration Inhibitory Factor is a Potential Target
10 516 for Discovery of Novel Anti-inflammatory Agents. *J. Biol. Chem.* 2002, 277, 24976-24982.
- 11 517 17. Senter, P. D.; Al-Abed, Y.; Metz, C. N.; Benigni, F.; Mitchell, R. A.; Chesney, J.; Han, J. L.;
12 518 Gartner, C. G.; Nelson, S. D.; Todaro, G. J.; Bucala, R., Inhibition of Macrophage Migration
13 519 Inhibitory Factor (MIF) Tautomerase and Biological Activities by Acetaminophen Metabolites.
14 520 *Proc. Natl. Acad. Sci. U.S.A.* 2002, 99, 144-149.
- 15 521 18. Winner, M.; Meier, J.; Zierow, S.; Rendon, B. E.; Crichlow, G. V.; Riggs, R.; Bucala, R.; Leng,
16 522 L.; Smith, N.; Lolis, E.; Trent, J. O.; Mitchell, R. A., A Novel Macrophage Migration Inhibitory
17 523 Factor Suicide Substrate Inhibits Motility and Growth of Lung Cancer Cells. *Cancer Res.* 2008,
18 524 68, 7253-7257.
- 19 525 19. Ouertatani-Sakouhi, H.; El-Turk, F.; Fauvet, B.; Roger, T.; Le Roy, D.; Karpinar, D. P.; Leng, L.;
20 526 Bucala, R.; Zweckstetter, M.; Calandra, T.; Lashuel, H. A., A New Class of Isothiocyanate-Based
21 527 Irreversible Inhibitors of Macrophage Migration Inhibitory Factor. *Biochemistry* 2009, 48,
22 528 9858-9870.
- 23 529 20. Xu, L.; Zhang, Y.; Zheng, L.; Qiao, C.; Li, Y.; Li, D.; Zhen, X.; Hou, T., Discovery of Novel
24 530 Inhibitors Targeting the Macrophage Migration Inhibitory Factor via Structure-based Virtual
25 531 Screening and Bioassays. *J. Med. Chem.* 2014, 57, 3737-3745.
- 26 532 21. Willett, P., Similarity-based Virtual Screening using 2D Fingerprints. *Drug Discov. Today* 2006,
27 533 11, 1046-1053.
- 28 534 22. Grethe, G.; Moock, T. E., Similarity Searching in REACCS. A New Tool for the Synthetic
29 535 Chemist. *J. Chem. Inf. Model.* 1990, 30, 511-520.
- 30 536 23. *Schrödinger, version 9.0; Schrödinger, LLC: New York, 2009.*
- 31 537 24. Lubetsky, J. B.; Swope, M.; Dealwis, C.; Blake, P.; Lolis, E., Pro-1 of Macrophage Migration
32 538 Inhibitory Factor Functions as a Catalytic base in the Phenylpyruvate Tautomerase Activity.
33 539 *Biochemistry* 1999, 38, 7346-7354.
- 34 540 25. Soares, T. A.; Goodsell, D. S.; Ferreira, R.; Olson, A. J.; Briggs, J. M., Ionization State and
35 541 Molecular Docking Studies for the Macrophage Migration Inhibitory Factor: the Role of Lysine
36 542 32 in the Catalytic Mechanism. *J. Mol. Recognit.* 2000, 13, 146-156.
- 37 543 26. Swope, M.; Sun, H. W.; Blake, P. R.; Lolis, E., Direct Link between Cytokine Activity and a
38 544 Catalytic Site for Macrophage Migration Inhibitory Factor. *EMBO J.* 1998, 17, 3534-3541.
- 39 545 27. Kaminski, G. A.; Friesner, R. A.; Tirado-Rives, J.; Jorgensen, W. L., Evaluation and
40 546 Reparametrization of the OPLS-AA Force Field for Proteins via Comparison with Accurate
41 547 Quantum Chemical Calculations on Peptides. *J. Phys. Chem. B* 2001, 105, 6474-6487.
- 42 548 28. Walters, W. P.; Stahl, M. T.; Murcko, M. A., Virtual Screening - an Overview. *Drug Discov.*
43 549 *Today* 1998, 3, 160-178.
- 44 550 29. Tian, S.; Li, Y.; Wang, J.; Xu, X.; Xu, L.; Wang, X.; Chen, L.; Hou, T., Drug-likeness Analysis of
45 551 Traditional Chinese Medicines: 2. Characterization of Scaffold Architectures for Drug-like
46 552 Compounds, Non-drug-like Compounds, and Natural Compounds from Traditional Chinese

- 1
2
3 553 Medicines. *J. Cheminformatics* **2013**, *5*, 5.
4 554 30. Tian, S.; Wang, J.; Li, Y.; Xu, X.; Hou, T., Drug-likeness Analysis of Traditional Chinese
5 555 Medicines: Prediction of Drug-likeness Using Machine Learning Approaches. *Mol. Pharmaceut.*
6 556 **2012**, *9*, 2875-2886.
7
8 557 31. Hou, T.; Wang, J.; Zhang, W.; Xu, X., ADME Evaluation in Drug Discovery. 7. Prediction of
9 558 Oral Absorption by Correlation and Classification. *J. Chem. Inf. Model.* **2007**, *47*, 208-218.
10 559 32. Cheng, K. F.; Al-Abed, Y., Critical Modifications of the ISO-1 Scaffold Improve its Potent
11 560 Inhibition of Macrophage Migration Inhibitory Factor (MIF) Tautomerase Activity. *Bioorg. Med.*
12 561 *Chem. Lett.* **2006**, *16*, 3376-3379.
13 562 33. Tao, L.; Zhang, F.; Hao, L.; Wu, J.; Jia, J.; Liu, J.-y.; Zheng, L. T.; Zhen, X.,
14 563 1-O-Tigloyl-1-O-deacetyl-nimbinin B Inhibits LPS-Stimulated Inflammatory Responses by
15 564 Suppressing NF- κ B and JNK Activation in Microglia Cells. *J. Pharmacol. Sci.* **2014**, *125*,
16 565 364-374.
17 566 34. Xu, Z.; Wu, J.; Zheng, J.; Ma, H.; Zhang, H.; Zhen, X.; Zheng, L. T.; Zhang, X., Design,
18 567 Synthesis and Evaluation of a Series of Non-steroidal Anti-inflammatory Drug Conjugates as
19 568 Novel Neuroinflammatory Inhibitors. *Int. Immunopharmacol.* **2015**, *25*, 528-537.
20 569 35. Zheng, L. T.; Hwang, J.; Ock, J.; Lee, M. G.; Lee, W.-H.; Suk, K., The Antipsychotic Spiperone
21 570 Attenuates Inflammatory Response in Cultured Microglia via the Reduction of Proinflammatory
22 571 Cytokine Expression and Nitric Oxide Production. *J. Neurochem.* **2008**, *107*, 1225-1235.
23 572 36. Bernhagen, J.; Mitchell, R. A.; Calandra, T.; Voelter, W.; Cerami, A.; Bucala, R., Purification,
24 573 Bioactivity, and Secondary Structure-Analysis of Mouse and Human Macrophage-Migration
25 574 Inhibitory Factor (MIF). *Biochemistry* **1994**, *33*, 14144-14155.
26 575 37. Calandra, T.; Bucala, R., Macrophage Migration Inhibitory Factor (MIF): A Glucocorticoid
27 576 Counter-regulator within the Immune System. *Crit. Rev. Immunol.* **1997**, *17*, 77-88.
28 577 38. Bernhagen, J.; Calandra, T.; Mitchell, R. A.; Martin, S. B.; Tracey, K. J.; Voelter, W.; Manogue,
29 578 K. R.; Cerami, A.; Bucala, R., MIF is a Pituitary-Derived Cytokine that Potentiates Lethal
30 579 Endotoxemia. *Nature* **1993**, *365*, 756-759.
31 580 39. West, P. W.; Parker, L. C.; Ward, J. R.; Sabroe, I., Differential and Cell-type Specific Regulation
32 581 of Responses to Toll-like Receptor Agonists by ISO-1. *Immunology* **2008**, *125*, 101-110.
33 582 40. Nathan, C., Nitric-Oxide as a Secretory Product of Mammalian-Cells. *FASEB J.* **1992**, *6*,
34 583 3051-3064.
35 584 41. Damas, P.; Ledoux, D.; Nys, M.; Vrindts, Y.; Degroote, D.; Franchimont, P.; Lamy, M., Cytokine
36 585 Serum Level During Severe Sepsis in Human IL-6 as a Marker of Severity. *Ann. Surg.* **1992**, *215*,
37 586 356-362.
38 587 42. Lappin, E.; Ferguson, A. J., Gram-positive Toxic Shock Syndromes. *Lancet Infect. Dis.* **2009**, *9*,
39 588 281-290.
40 589 43. Alcaraz, M. J.; Fernandez, P.; Guillen, M. I., Anti-inflammatory Actions of the Heme
41 590 Oxygenase-1 Pathway. *Curr. Pharm. Des.* **2003**, *9*, 2541-2551.
42 591 44. Ryter, S. W.; Alam, J.; Choi, A. M. K., Heme Oxygenase-1/carbon Monoxide: from Basic
43 592 Science to Therapeutic Applications. *Physiol. Rev.* **2006**, *86*, 583-650.
44 593 45. Carchman, E. H.; Rao, J.; Loughran, P. A.; Rosengart, M. R.; Zuckerbraun, B. S., Heme
45 594 Oxygenase-1-Mediated Autophagy Protects Against Hepatocyte Cell Death and Hepatic Injury
46 595 from Infection/Sepsis in Mice. *Hepatology* **2011**, *53*, 2053-2062.
47 596 46. Tamion, F.; Richard, V.; Renet, S.; Thuillez, C., Intestinal Preconditioning Prevents Inflammatory

- 1
2
3 597 Response by Modulating Heme Oxygenase-1 Expression in Endotoxic Shock Model. *Am. J.*
4 598 *Physiol. Gastrointest. Liver Physiol.* **2007**, *293*, G1308-G1314.
5 599 47. Calandra, T.; Roger, T., Macrophage Migration Inhibitory Factor: a Regulator of Innate
6 600 Immunity. *Nature Rev. Immunol.* **2003**, *3*, 791-800.
7
8 601 48. Riedemann, N. C.; Guo, R. F.; Ward, P. A., Novel Strategies for the Treatment of Sepsis. *Nature*
9 602 *Med.* **2003**, *9*, 517-524.
10 603 49. Rittirsch, D.; Flierl, M. A.; Ward, P. A., Harmful Molecular Mechanisms in Sepsis. *Nature Rev.*
11 604 *Immunol.* **2008**, *8*, 776-787.
12
13 605 50. Yoshimoto, T.; Nakanishi, K.; Hirose, S.; Hiroishi, K.; Okamura, H.; Takemoto, Y.; Kanamaru,
14 606 A.; Hada, T.; Tamura, T.; Kakishita, E., High Serum IL-6 Level Reflects Susceptible Status of the
15 607 Host to Endotoxin and IL-1/tumor necrosis Factor. *J. Immunol.* **1992**, *148*, 3596-3603.
16
17 608 51. Miyashita, T.; Kakimoto, N.; Ishida, Y.; Hayashi, T.; Kimura, A.; Tsokos, M.; Kondo, T.,
18 609 Immunohistochemical Expression of Tumor Necrosis Factor-alpha in Sepsis-induced Lung Injury.
19 610 *Forensic. Sci. Med. Pathol.* **2006**, *2*, 103-108.
20 611
21 612
22 613
23 614
24 615
25 616
26 617
27 618
28 619
29 620
30 621
31 622
32 623
33 624
34 625
35 626
36 627
37 628
38 629
39 630
40 631
41 632
42 633
43 634
44 635
45 636
46 637
47 638
48 639
49 640
50
51
52
53
54
55
56
57
58
59
60

1
2
3
4
5
6
7
8
9
10
11
12
13
14
15
16
17
18
19
20
21
22
23
24
25
26
27
28
29
30
31
32
33
34
35
36
37
38
39
40
41
42
43
44
45
46
47
48
49
50
51
52
53
54
55
56
57
58
59
60

641 **Legend of the figures**

642 **Figure 1.** The binding pockets of MIF for compounds (a) **5**, (b) **8**, (c) **13**, and (d) **15**.

643 **Figure 2.** (a-d) Concentration-dependent inhibition of MIF tautomerase activity by
644 three active molecules. (e-f) Three compounds were chosen to measure iNOS
645 expression and TNF- α release based on the inhibitory effect both on tautomerse
646 activity and NO production. All compounds show protective effect in LPS-stimulated
647 RAW 264.7 macrophages, with compound **5** of them exhibiting the highest potency.

648 **Figure 3.** Effects of compound **5** on the production of nitric oxide (NO), TNF- α and
649 IL-6 in LPS-activated RAW 264.7 macrophage cells. RAW 264.7 macrophage cells
650 were pretreated with or without the indicated concentration (1-25 μ M) of compound **5**
651 for 30 min, followed by LPS (50 ng/mL) treatment for 24 h. (a) Amounts of NO in the
652 culture supernatants were measured using Griess reagent. (b) Cell viability was
653 determined by MTT assay. (c) The amounts of TNF- α and (d) IL-6 in the supernatants
654 were measured using ELISA respectively. The data were expressed as percentage of
655 surviving cells over control cells. The data are the mean \pm SD of 3 independent
656 experiments. * $p < 0.05$, ** $p < 0.01$, *** $p < 0.001$ compared with LPS only group.

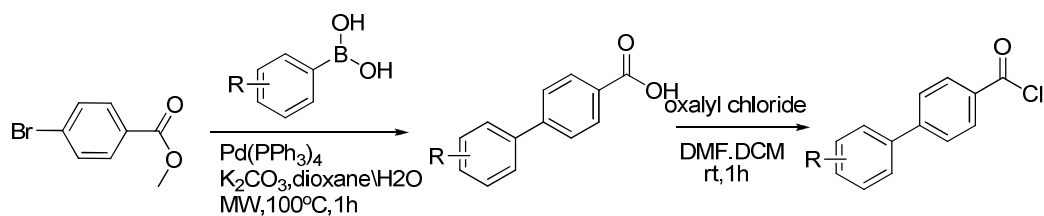
657 **Figure 4.** Effects of compound **5** on gene expression of proinflammatory factors and
658 HO-1 in LPS-treated RAW 264.7 macrophages cells. RAW 264.7 macrophages cells
659 were treated with compound **5** (1-25 μ M) for 30 min, followed by LPS (50 ng/mL)
660 treatment. (a-f) After 6 h of LPS stimulation, the mRNA levels of iNOS, IL-6, TNF- α ,
661 COX-2, IL-1 β and HO-1 were determined by quantitative real-time PCR assay. After
662 16 h of LPS stimulation, the protein levels of iNOS, COX-2 and MIF were
663 determined by western blotting using respective primary antibodies. (g) The α -tubulin
664 was used as an internal control. Quantification of protein expression was performed
665 by densitometric analysis. (h) The data are the mean \pm SD of 3 independent
666 experiments. * $p < 0.05$, ** $p < 0.01$, *** $p < 0.001$ compared with LPS only group.

667 **Figure 5.** Effects of compound **5** on LPS-induced endotoxic shock. (a) Male Balb/C
668 mice were injected compound **5** (i.p. intraperitoneal injection) at indicated doses or
669 vehicle 1 h prior to administration of LPS (4.5 mg/kg, i. p.) for 3 days. Survival was

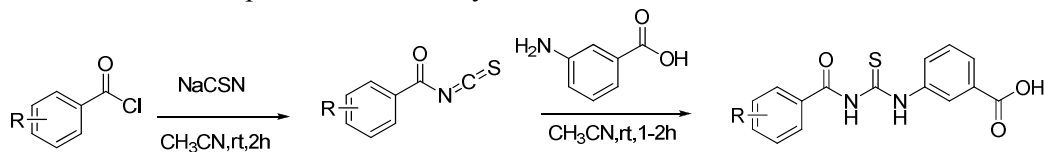
1
2
3
4 670 monitored for 6 days. ($n = 20$ for each group). (b) Mice were pretreated with
5
6 671 compound **5** (1, 0.5 mg/kg, i.p.) or vehicle 1 h prior to the administration of LPS (4.5
7
8 672 mg/kg, i.p.). Serum was collected at 12 h post-injection of LPS. The serum level of
9
10 673 TNF- α and IL-6 were measured using ELISA. Data are presented as means \pm SD ($n =$
11
12 674 6 for each group). * $p < 0.05$, ** $p < 0.01$, *** $p < 0.001$ compared with LPS only
13
14 675 group. (c) Mice were pretreated compound **5** (1, 0.5 mg/kg, i.p.) or vehicle 1 h prior to
15
16 676 the administration of LPS (4.5 mg/kg, i.p.). 12 h after LPS challenge, mice were
17
18 677 sacrificed to obtain lung tissue for histological analysis. (d) H&E staining was
19
20 678 performed using lung tissue specimens from vehicle LPS + vehicle, LPS + 1 mg/kg
21
22 679 compound **5**, LPS + 0.5mg/kg compound **5**, mice, respectively (Magnification 400 \times).
23
24
25
26
27
28
29
30
31
32
33
34
35
36
37
38
39
40
41
42
43
44
45
46
47
48
49
50
51
52
53
54
55
56
57
58
59
60

1
2
3
4
5
6
7
8
9
10
11
12
13
14
15
16
17
18
19
20
21
22
23
24
25
26
27
28
29
30
31
32
33
34
35
36
37
38
39
40
41
42
43
44
45
46
47
48
49
50
51
52
53
54
55
56
57
58
59
60

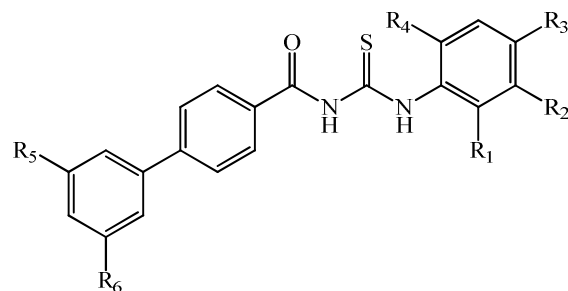
700 **Scheme 1.** General procedure for the synthesis of **12-14**.



Scheme 2. General procedure for the synthesis of **35-42**.



736 **Table 1.** Experimentally determined half-maximal inhibitory concentrations (IC₅₀) of
 737 MIF tautomerase activity (TIC₅₀) for biphenyl series, and NO production of
 738 compounds with TIC₅₀ < 10 μM in LPS-activated RAW 264.7 macrophage (NIC₅₀).



739

740

No.	R ₁	R ₂	R ₃	R ₄	R ₅	R ₆	TIC ₅₀ (μM)	NIC ₅₀ (μM)
1	H	carboxy	H	H	H	H	0.72 ± 0.15	36.02 ± 1.56
2	H	carboxy		methyl	H	H	4.25 ± 0.63	49.93 ± 1.70
3	H	H	carboxy	H	H	H	11.66 ± 1.07	
4	H	H	acetylamino	H	H	H	6.25 ± 0.80	33.51 ± 1.53
5	H	H	hydroxy	H	H	H	0.37 ± 0.09	4.26 ± 0.63
6	H	H	carbomethoxy	H	H	H	20.42 ± 1.31	
7	H	hydroxymethyl	H	H	H	H	8.42 ± 0.93	25.57 ± 1.41
8	H	carboxy	H	Cl	H	H	0.71 ± 0.15	23.77 ± 1.38
9	carbomethoxy	H	H	H	H	H	8.36 ± 0.92	26.57 ± 1.42
10	H	carboxy	H	methoxyl	H	H	5.53 ± 0.74	12.05 ± 1.08
11	H	acetyl	H	H	H	H	8.63 ± 0.94	13.10 ± 1.12
12*	H	carboxy	H	H	trifluoromethyl	trifluoromethyl	1.48 ± 0.17	20.71 ± 1.32
13*	H	carboxy	H	H	Cl	Cl	0.96 ± 0.02	23.24 ± 1.37
14*	H	carboxy	H	H	F	F	2.48 ± 0.39	28.08 ± 1.45

741 *Synthesized compounds

742

743

744

745

746

747

748

749

750

751

752

753

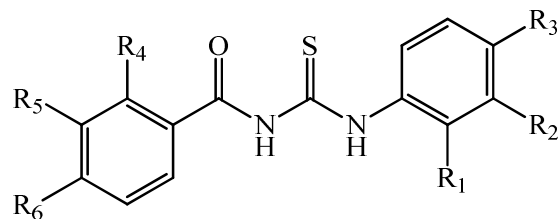
754

755

756

757

Table 2. Experimentally determined half-maximal inhibitory concentrations (IC_{50}) of MIF tautomerase activity (TIC_{50}) for benzene series, and NO production of compounds with $TIC_{50} < 10 \mu M$ in LPS-activated RAW 264.7 macrophage (NIC_{50}).

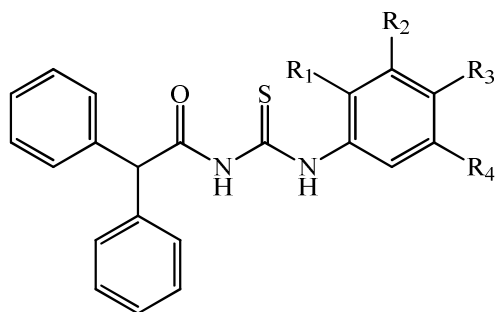


No.	R ₁	R ₂	R ₃	R ₄	R ₅	R ₆	TIC_{50} (μM)	NIC_{50} (μM)
15	H	carboxy	H	H	H	methyl	0.66 ± 0.18	12.61 ± 1.10
16	H	H	carboxy	H	H	methyl	1.33 ± 0.37	25.70 ± 1.41
17	methyl	carboxy	H	H	H	phenoxyethyl	6.67 ± 0.82	45.98 ± 1.66
18	H	H	carboxy	H	H	H	9.77 ± 0.99	59.74 ± 1.78
19	methyl	carboxy	H	H	H	isopropyl	8.63 ± 0.94	25.82 ± 1.41
20	H	H	carboxy	H	methyl	H	28.33 ± 1.45	
21	H	Cl	carboxy	H	H	F	39.06 ± 1.59	
22	H	acetyl	H	H	H	H	2.74 ± 0.44	16.39 ± 1.21
23	H	H	carbomethoxy	methyl	H	H	>100	
24	H	H	carbomethoxy	H	H	H	4.65 ± 0.67	40.35 ± 1.61
25	H	H	acetyl	H	H	H	2.73 ± 0.44	17.06 ± 1.23
26	H	H	carbomethoxy	H	methyl	H	64.94 ± 1.81	
27	H	H	benzamido	H	H	methyl	3.75 ± 0.57	32.52 ± 1.52
28	H	H	carbomethoxy	H	H	H	13.18 ± 1.12	
29	H	H	acetylamino	H	methyl	H	10.39 ± 1.02	
30	H	H	carbomethoxy	H	carbomethoxy	H	8.43 ± 0.93	17.13 ± 1.23
31	H	H	carbomethoxy	H	H	carbomethoxy	5.00 ± 0.70	20.85 ± 1.32
32	H	H	acetylamino	H	H	methyl	10.58 ± 1.02	
33	carbomethoxy	H	H	H	H	methyl	0.81 ± 0.09	55.24 ± 1.74
34	carbomethoxy	H	H	H	methyl	H	0.77 ± 0.11	45.23 ± 1.66
35*	H	carboxy	H	H	H	Br	16.69 ± 1.22	
36*	H	carboxy	H	H	H	trifluoromethyl	21.01 ± 1.32	
37*	H	carboxy	H	H	H	Cl	24.25 ± 1.39	
38*	H	carboxy	H	H	H	F	26.26 ± 1.42	
39*	H	carboxy	H	H	F	H	12.23 ± 1.09	
40*	H	carboxy	H	H	Cl	H	28.71 ± 1.46	
41*	H	carboxy	H	Cl	H	H	61.15 ± 1.79	
42*	H	carboxy	H	F	H	H	>100	

*Synthesized compounds

1
2
3
4
5
6
7
8
9
10
11
12
13
14
15
16
17
18
19
20
21
22
23
24
25
26
27
28
29
30
31
32
33
34
35
36
37
38
39
40
41
42
43
44
45
46
47
48
49
50
51
52
53
54
55
56
57
58
59
60

768 **Table 3.** Experimentally determined half-maximal inhibitory concentrations (IC₅₀) of
769 MIF tautomerase activity (TIC₅₀) for diphenylmethane series, and NO production of
770 compounds with TIC₅₀ < 10 μM in LPS-activated RAW 264.7 macrophage (NIC₅₀).
771



772
773

No.	R ₁	R ₂	R ₃	R ₄	TIC ₅₀ (μM)	NIC ₅₀ (μM)
43	H	H	carboxy	H	13.55 ± 1.13	
44	H	carboxy	H	H	7.95 ± 0.90	59.74 ± 1.78
45	H	H	H	H	6.67 ± 0.82	22.50 ± 1.35
46	H	H	carbomethoxy	H	5.51 ± 0.74	13.43 ± 1.13
47	H	H	benzamido	H	2.74 ± 0.44	12.57 ± 1.10
48	H	H	formylamino	H	19.80 ± 1.30	
49	carbomethoxy	H	H	H	8.70 ± 0.94	18.66 ± 1.27
50	H	carbomethoxy	H	carbomethoxy	3.63 ± 0.56	9.33 ± 0.97
51	H	H	phenylamino	H	1.43 ± 0.15	15.51 ± 1.19

774
775
776
777
778
779
780
781
782
783
784
785
786
787
788
789
790
791
792
793
794

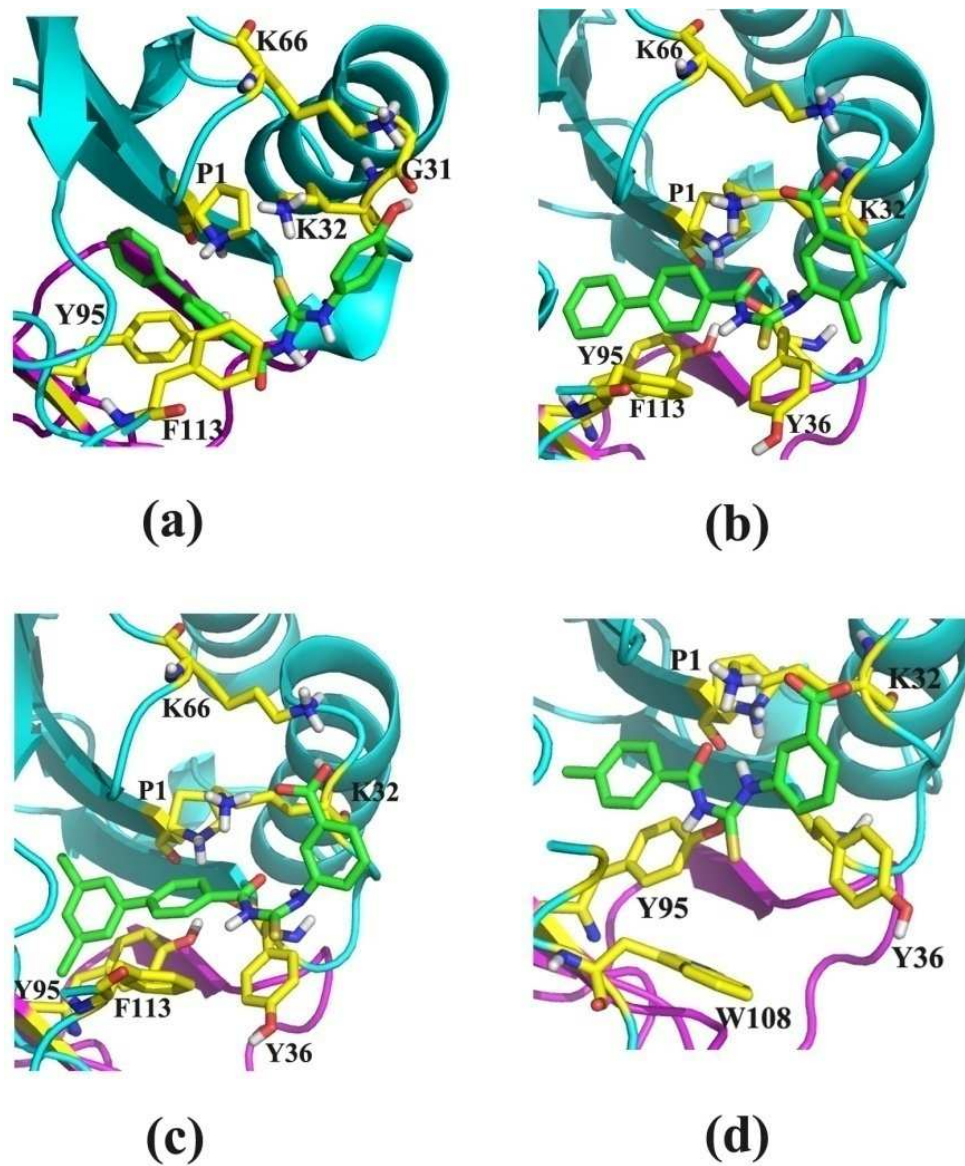
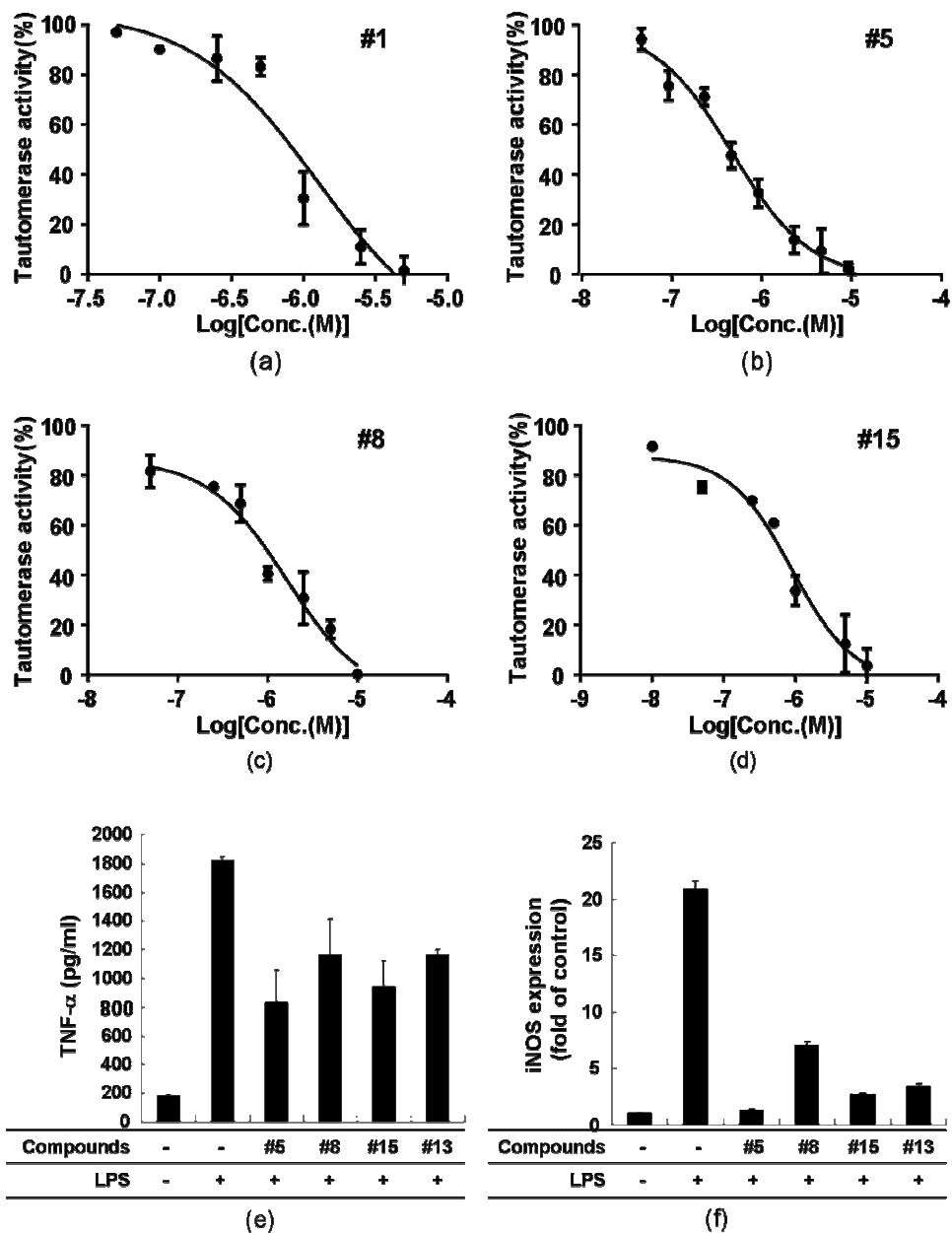


Figure 1

795
796
797
798
799
800
801
802
803
804
805
806
807
808



809

810

811

812

Figure 2

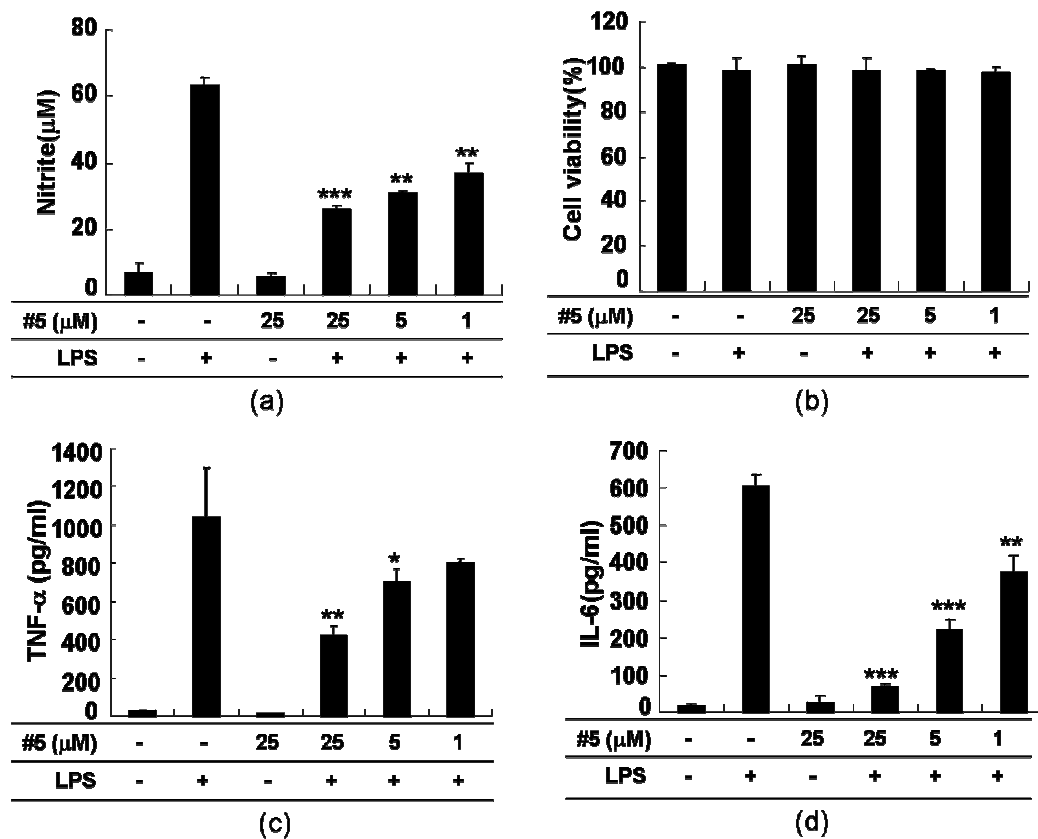


Figure 3

813
814
815
816
817
818
819
820
821
822
823
824
825
826
827
828
829
830
831
832
833
834

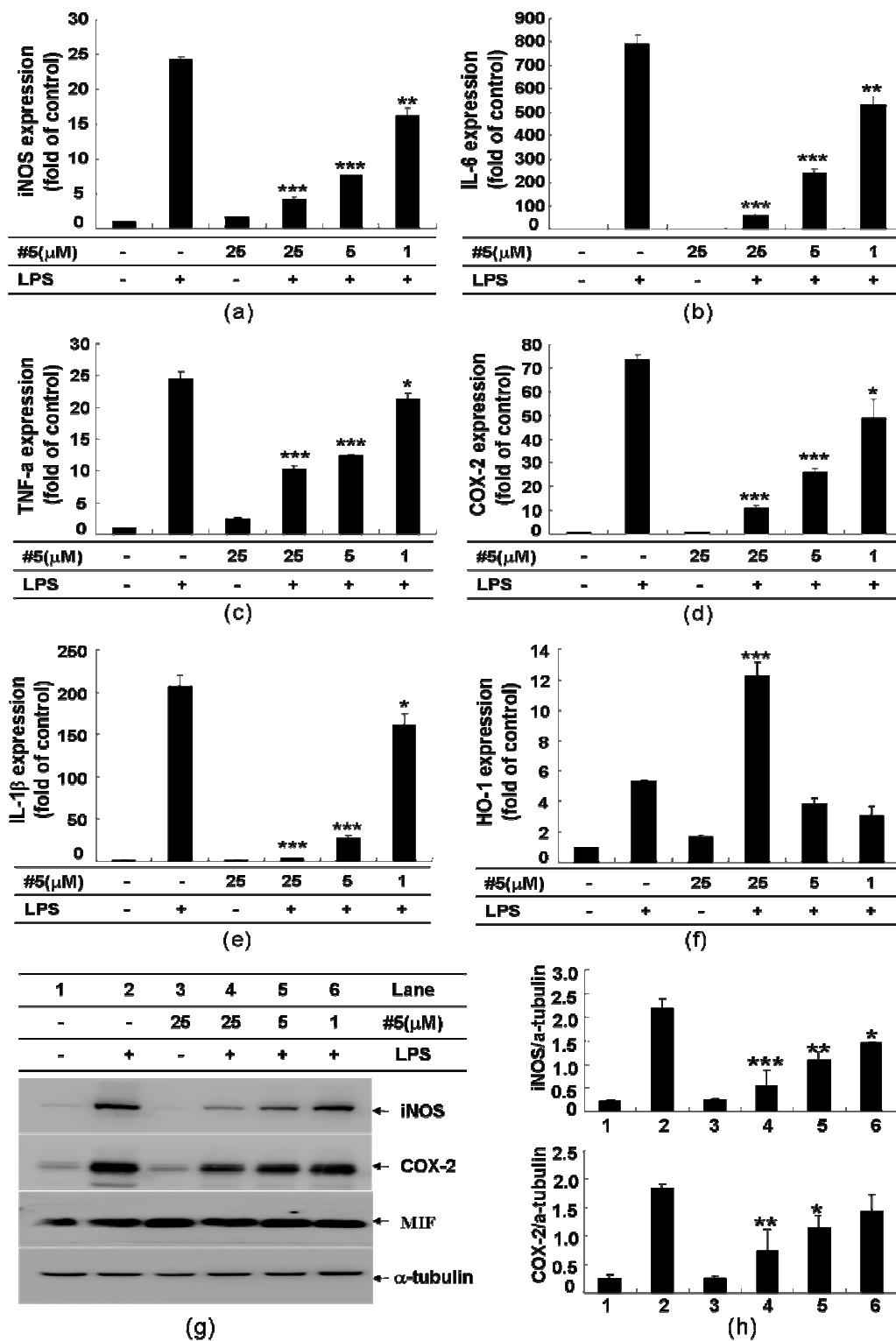
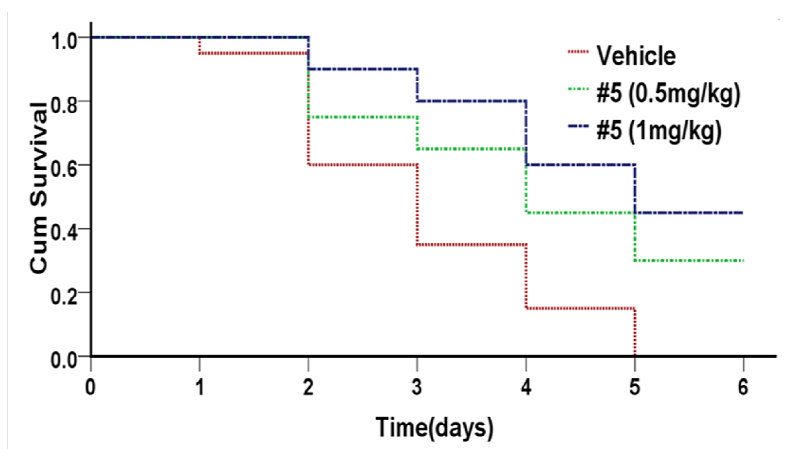


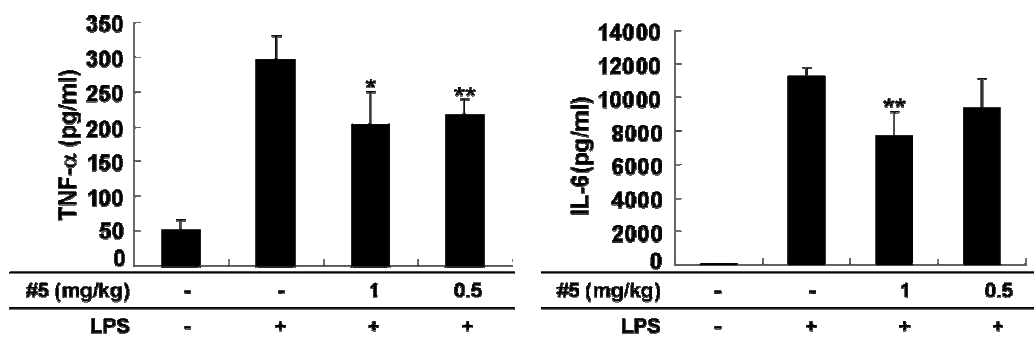
Figure 4

835

836

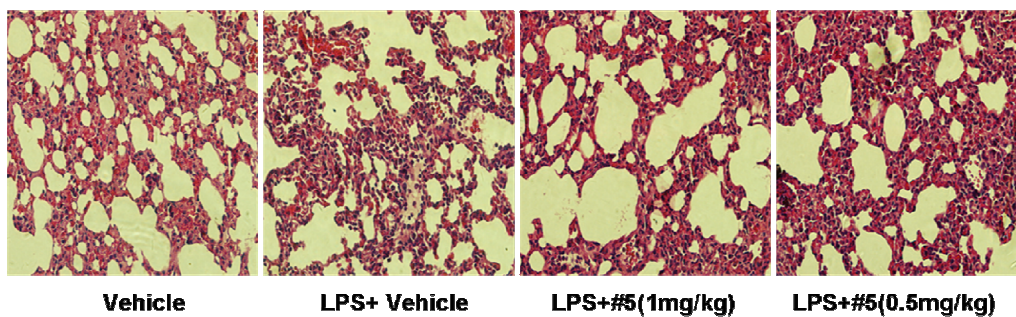


(a)



(b)

(c)



(d)

Figure 5

837

838

839